Indian J. Fish., 73 (1): 83-96, 2026 doi:10.21077/ijf.2026.73.1.163941-10

Available online at: epubs.icar.org.in/index.php/IJF

Comparative analysis of MHC class II A gene in *Trachinotus mookalee* and *Trachinotus blochii*: Molecular identification and *in silico* characterisation

C. Lavina-Vincent[1,2], Sandhya Sukumaran[1], V. G. Vysakh[1], Wilson Sebastian[1] Shubhadeep Ghosh[3], Grinson George[1] and A. Gopalakrishnan[1*]

[1]ICAR-Central Marine Fisheries Research Institute, Kochi-682 018, Kerala, India
[2]Mangalore University, Mangalagangotri, Mangaluru-574 199, Karnataka, India
[3]Krishi Anusandhan Bhavan-II, Indian Council of Agricultural Research, Pusa-110 012, New Delhi, India

Abstract

Trachinotus mookalee and *Trachinotus blochii* are the two commercially important pompano species successfully farmed in aquaculture, and are susceptible to various infectious diseases. As in higher vertebrates, the major histocompatibility complex (MHC) gene superfamily plays crucial role in the adaptive immunity of teleost fishes by mediating the recognition and presentation of pathogen derived antigens to T cells, thereby contributing to disease resistance. The present study reports the identification and *in silico* characterisation of the MHC class II A gene in *T. mookalee* (*Trmo-DAA*) and *T. blochii* (*Trbl-DAA*). The coding region of the target gene in both species was 1026 bp in length, comprising 4 exons and encoding a polypeptide of 241 amino acids. Phylogenetic analysis revealed that the MHC II A gene of *T. blochii* is more closely related to *Trachinotus ovatus* than to *T. mookalee*. *In silico* analysis highlighted that the target gene is involved in the processing and presentation of exogenous antigen, as supported by domain and motif prediction, Gene Ontologies (GO) annotation, Kyoto Encyclopedia of Genes and Genomes (KEGG) pathway analysis and STRING-based protein-protein interaction networks. The predicted secondary structure (2D) majorly comprised random coils and β strands, while the tertiary structure (3D) showed the highest similarity to the MHC class II A protein of *Lates calcarifer*. Ramachandran plot validation suggested that the predicted 3D structure of *Trbl-DAA* exhibits better stereochemical stability than that of *Trmo-DAA*. These findings provide valuable insights into the molecular and structural characteristics of MHC class II A genes in *Trachinotus* species and may support future studies on disease resistance and selective breeding.

*Correspondence e-mail:
agopalkochi@gmail.com

Keywords:
Disease resistance, Indian pompano, Silver pompano, Snubnose pompano, *Trmo-DAA, Trbl-DAA*

Received : 20.01.2025
Accepted : 23.12.2025

Introduction

Species of the genus *Trachinotus* (family Carangidae), commonly referred to as pompano, are widely distributed in the temperate, tropical and subtropical waters. *Trachinotus mookalee* (Indian pompano) is distributed from the western Indian Ocean to the western Pacific Ocean and is considered an ideal candidate for marine and estuarine cage culture systems, owing to its rapid growth, readiness to accept artificial feed and high adaptability to cage farming conditions (Sekar *et al.*, 2021). *Trachinotus blochii* (Silver pompano/ Snubnose pompano) is another commercially important species valued for its attractive appearance, fast and uniform growth rate, adaptability to culture environment, suitability to formulated feeds, firm white flesh with desirable taste as well as high domestic and international market demand. The aquaculture of silver pompano has been successfully established in many Asia–Pacific countries such as China, Taiwan and Indonesia (Chavez *et al.*, 2011). Recent attainments in broodstock development, breeding and seed production of these species further highlight their potential for sustainable aquaculture expansion (Gopakumar *et al.*, 2012). However, intensive farming practices and eutrophic water conditions have led to the occurrence of several disease outbreaks in these fishes, including infections caused by Betanodavirus (Ransangan *et al.*, 2011;

Yang *et al*., 2022); *Streptococcus agalactiae* (Amal *et al.*, 2012) and *Amyloodinium ocellatum* (Kumar *et al.*, 2015).

The innate and acquired immune systems of teleost fishes are well developed and function in a coordinated manner to defend against pathogens. As in higher vertebrates, the major histocompatibility complex (MHC) plays a crucial role by processing and presenting self and non-self antigens to T cell receptors (TCR), triggering immune response. The MHC is classified into two major classes *i.e.* class I and class II, each with distinct roles in antigen presentation. Structurally, the MHC class II molecule is a heterodimer of α and β chains (Brown *et al.*, 1993), each comprising a membrane distal extracellular domain (α1 or β1), a membrane proximal extracellular domain (α2 or β2), a transmembrane region, and a short cytoplasmic anchor (Rothbard and Gefter, 1991). The α and β chains are encoded by the genes A and B, respectively (Klein and Figueroa, 1986). The peptide binding region (PBR) formed by the α1 and β1 domains, is the most functionally important part of the molecule that interacts with antigenic peptides. This region exhibits the highest degree of polymorphism, particularly in exon 2 which encodes the PBR, facilitating a broad range of antigen recognition (Apanius *et al.*, 1997). MHC class II molecules are predominantly expressed on antigen-presenting cells such as macrophages, dendritic-like cells and B cells, further emphasising their critical role in adaptive immunity.

The MHC II genes have been characterised in various bony fish species such as rainbow trout (Glamann, 1985), salmon (Hordvik *et al.*, 1993; Grimholt *et al.*, 2003), zebrafish (Ono *et al.*, 1992; Sultmann *et al.*, 1993), carp (Van Erp *et al.*, 1996), striped bass (Walker and McConnell, 1994; Hardee *et al.*, 1995), half-smooth tongue sole (Xu *et al.*, 2009 ; Li *et al.*, 2010), miiuy croaker (Xu *et al.*, 2011), stone flounder (Jiang *et al.*, 2013), tilapia (Sato *et al.*, 2012; Pang *et al.*, 2013; Zhou *et al.*, 2013), medaka (Bannai and Nonaka, 2013), spotted halibut (Li *et al.*, 2011), olive flounder (Srisapoome *et al.*, 2004) , turbot (Zhang and Chen, 2006), large yellow croaker (Yu *et al.*, 2010), channel catfish (Godwin *et al.*, 1997) and European seabass (Buonocore *et al.*, 2007). In teleosts, MHC polymorphism has been linked to resistance or susceptibility to various viral and bacterial diseases (Gjedrem *et al.*, 1991; Grimholt *et al.*, 1994, 2003; Lohm *et al.*, 2002; Glover *et al.*, 2007; Wynne *et al.*, 2007; Rakus *et al.*, 2009a, b; Xu *et al.*, 2009, 2010; Spurgin and Richardson, 2010; Eizaguirre *et al.*, 2012; Zhu *et al.*, 2018). Studies have confirmed associations between MHC class II A alleles and resistance or susceptibility to bacterial or viral infections, suggesting that MHC markers could be applied in marker-assisted selective breeding for disease resistance (Yang *et al.*, 2016a, b; Li *et al.*, 2017; Cao *et al.*, 2018; Chen *et al.*, 2021).

Despite these advancements, the molecular identification, characterisation and analysis of the MHC class II α chain coding region have not yet been reported in *T. mookalee* and *T. blochii*. Therefore, the present study aimed to identify and characterise the MHC class II A gene and to elucidate their structural and functional properties through *in silico* analyses in these two species. According to the nomenclature system proposed by Klein *et al.* (1990), MHC class II α and β chain genes are designated as *DAA* and *DAB*, respectively. Following this standardised system, species-specific prefixes *viz., Trmo-* for *T. mookalee* and *Trbl-* for *T. blochii*, were used to ensure consistency in comparative and evolutionary analyses across teleosts. Accordingly, the MHC II A genes in *T. mookalee* and *T. blochii* are designated as *Trmo-DAA* and *Trbl-DAA*, respectively. Comprehensive *in silico* sequence analyses, including sequence characterisation and secondary (2D) as well as tertiary (3D) structure predictions were performed to investigate the molecular, structural and functional properties of these genes, providing insights into their potential roles in immune defense.

Materials and methods

Sample collection

Tissue samples were collected from healthy adult specimens of *T. mookalee* (total length: 48.9 cm and weight: 1412 g) and *T. blochii* (total length: 41.5 cm and weight: 1100 g), both of similar age (2 years). The specimens were obtained from the marine finfish hatchery of the ICAR-Central Marine Fisheries Research Institute (ICAR-CMFRI) Regional Centre, Vishakhapatnam and the ICAR-CMFRI Regional Centre, Vizhinjam, respectively. The fish were transported alive to the laboratory and maintained under standard conditions of salinity, pH, temperature and dissolved oxygen. Prior to sampling, the fish were euthanised using a clove oil solution. Subsequently, the fish were dissected and muscle tissues were collected using sterile scissors and forceps under aseptic conditions. The collected tissues were preserved in RNA later for RNA isolation and in 100% ethanol for DNA isolation. The samples were stored at -20°C until further processing.

Primer designing, genomic DNA isolation and PCR amplification

Six primers (Table 1) were designed based on conserved regions of the MHC II A gene of *T. ovatus*. Primer3 (v.0.4.0) (https://bioinfo.ut.ee/primer3-0.4.0/) was used to design the primers that cover the exons and introns in the genomic DNA. The Phenol-Chloroform method (Sambrook and Russell, 2001) was used to extract total genomic DNA from the samples. The quality and integrity of the extracted DNA were evaluated by 0.8% agarose gel electrophoresis, while the concentration and purity were determined using a NanoDrop 2000 spectrophotometer (Thermo Fisher Scientific, USA). DNA samples showing intact, high molecular weight bands on the gel and an OD_{260}/OD_{280} ratio of ~1.8 were considered suitable for downstream analyses. The purified and intact genomic DNA was used as a template for PCR amplification. The PCR reaction was carried out in a total volume of 25 µl, containing 2.5 µl of 10x Taq buffer, 0.2 mM dNTPs, 0.2 µM of each primer, 1.5 U of Taq DNA polymerase (Sigma-Aldrich, USA), and 1 µl of template DNA (1000 ng μl^{-1}), with the final volume adjusted using nuclease-free water. PCR amplification was carried out under the following conditions: initial denaturation at 94°C for 4 min, 35 cycles of denaturation at 94°C for 30 s, annealing at the temperatures given in Table 1 for 30 s, and extension at 72°C for 30 s, followed by a final extension at 72°C for 10 min. The amplified PCR products were analysed on a 1.2% agarose gel to verify the expected amplicon sizes. PCR products were subsequently sequenced using the Sanger sequencing method and the resulting sequences assembled into contigs and overlapping regions were aligned using SeqMan Pro 7.1 software to generate the final *Trmo-DAA* and *Trbl-DAA* sequences.

Table 1. Details of the primers designed and used in the present study

Primer name	Sequence (5' to 3')	Annealing temperature (Tm, °C)	Product size (bp)	Application
MHC II A FP1	CTTTCAGAGACCTGCTGCTG	62	463	Genomic DNA and cDNA amplification
MHC II A RP1	TCCAGTGGGATGTCCTTCAT			
MHC II A FP2	TCAACCACAGAGGAGTCGAG	62	1105	"
MHC II A RP2	ACTTTGACGGGAGCAGGGTA			
MHC II A FP3	CTCCTTCCAGTCCAGTCGTC	62	458	"
MHC II A RP3	ACAGGAGCGAAGCTGTTTCC			

RNA isolation and cDNA synthesis

Total RNA was isolated from samples preserved in RNAlater using TRI Reagent® (Sigma-Aldrich, USA), as per the manufacturer's protocol. The quality and integrity of the isolated RNA were assessed on a 1% agarose gel, while RNA concentration and purity were determined using a Nanodrop 2000 spectrophotometer (Thermo Fisher Scientific, USA) based on the OD 260/280 ratio. First-strand cDNA was synthesised using the PrimeScript™ 1st strand cDNA synthesis kit (Takara, Japan) in a 20 µl reaction volume with 2 µg of total RNA. The synthesised cDNA was subsequently sequenced using the Sanger sequencing method to obtain the coding regions of the target genes. The exon-intron boundaries of the genes were characterised by aligning the cDNA sequences with the corresponding genomic DNA sequences.

Sequence alignment and phylogenetic analysis

The amino acid sequences of *Trmo-DAA* and *Trbl-DAA* were subjected to multiple alignment using CLUSTAL-W, followed by phylogenetic analysis using MEGA 7.0 software (http://www.megasoftware.net). A maximum likelihood (ML) phylogenetic tree was built based on the best fit amino acid substitution model, identified as the Whelan and Goldman (WAG) model with gamma distributed rate variation among sites and supported by 1000 bootstrap replicates.

In silico sequence analysis

The complete coding region of *Trmo-DAA* and *Trbl-DAA* were submitted to the NCBI-Genbank database to obtain the accession numbers. The physico-chemical\properties of the encoded proteins, including molecular weight, theoretical isoelectric point (pI), instability index, amphipathic index and GRAVY (grand average of hydropathy) score were calculated using the ExPasy ProtParam Tool (http://web.expasy.org/protparam/). The potential phosphorylation and N-linked glycosylation sites were predicted using NetPhos-3.1 server (https://services.healthtech.dtu.dk/services/NetPhos-3.1/) and NetNGlyc1.0 server (https://services.healthtech.dtu.dk/services/NetNGlyc-1.0/), respectively. The subcellular localisation of the proteins was predicted using PSORT-II (https://psort.hgc.jp/). Protein family classification along with the identification of functional domains, motifs, signal peptides and repeat regions were performed using InterProScan (https://www.ebi.ac.uk/interpro/search /sequence/). The open reading frames (ORFs) of both *Trmo-DAA* and *Trbl-DAA* were used as input in the STRING database (https://string-db.org/) to predict protein–protein interaction networks. Functional enrichment analyses, including Gene Ontologies (GO) and Kyoto Encyclopedia of Genes and Genomes (KEGG) pathways were carried out by comparison with homologous proteins from the model organism *Danio rerio*.

In silico structure analysis

The presence of signal peptides and transmembrane topology of *Trmo-DAA* and *Trbl-DAA* proteins were predicted using Phobius (https://phobius.sbc.su.se/). The online tool Protter (https://wlab.ethz.ch/protter/start/), was used to generate interactive visualisations of the transmembrane regions and protein topology. Secondary structure prediction was performed using the PSIPRED Protein Analysis Workbench version 4.0 (http://bioinf.cs.ucl.ac.uk/psipred/), developed by the UCL-CS Bioinformatics. Three-dimensional (3D) structures of the proteins were predicted by homology modelling using SWISS-MODEL (https://swissmodel.expasy.org/). Template search for the query *Trmo-DAA* and *Trbl-DAA* amino acid sequences was performed and the sequence having the highest identity with the query sequences was selected as the template for homology modelling.

The protein structure prediction server PHYRE-2.2 (https://www.sbg.bio.ic.ac.uk/phyre2/) (Powell *et al.*, 2025) was also used to generate 3D models based on remote homology detection and threading. The *Trmo-DAA* and *Trbl-DAA* amino acid sequences were analysed using PSI-BLAST to detect remote sequence homologues and suitable template structures. The 3D structure of the template was obtained by threading the aligned sequences, which matches with the amino acid sequence of the known high-quality AlphaFold model in AlphaFold Protein Structure Database. From the list of top 20 template matches generated, the first one with the highest sequence identity and highest confidence score was selected for subsequent structural quality assessment and functional analysis of the 3D structure.

Results and discussion

Trmo-DAA and *Trbl-DAA* coding regions in *T. mookalee* and *T. blochii*

The MHC II A sequences of *T. mookalee* (*Trmo-DAA*) and *T. blochii* (*Trbl-DAA*) were submitted to the NCBI GenBank, under accession numbers PQ729892 and PQ729893, respectively. The coding region in both species was 1026 bp long, comprising 4 exons and encoding a polypeptide chain of 241 amino acids (Fig. 1a, b). The first exon (exon 1), encoding the leader peptide was 70 bp long, while exons 2 and 3 encoding the α_1 and α_2 domains of the protein were 249 bp and 285 bp in length respectively. Exon 4 which encodes connecting

peptide, transmembrane domain and cytoplasmic domain, was 122 bp long in both the species. Similar to other teleost species, *Trmo-DAA* and *Trbl-DAA* consisted of a leader peptide, two extracellular domains (α_1 and α_2) and a transmembrane or cytoplasmic domain (Zhang *et al.*, 2006; Pang *et al.*, 2013). The exon sizes and intron-exon boundaries were nearly identical to the MHC II A gene of *T. ovatus* (Cao *et al.*, 2018). The lenghts of exons 2, 3 and 4 are generally similar in most of the teleost MHC II A genes, while variation is primarily observed in exon 1 which encodes the leader peptide (Xu *et al.*, 2010; 2011; Yu *et al.*, 2010; Li *et al.*, 2011).

Multiple alignment and phylogenetic analysis

The MHC II A amino acid sequences from different teleost fishes were subjected to multiple sequence alignment (Fig. 2) and pairwise distance calculated showed that the sequences of *T. blochii (Trbl-DAA)* was more similar to *T. ovatus* (95%) than to *T. mookalee (Trmo-DAA),* which displayed 93% similarity. The coding regions of the candidate genes contained 16 variable amino acid sites caused by non-synonymous substitutions. The sequences also showed 80% similarity with the MHC II A sequences from *Seriola aureovittata*

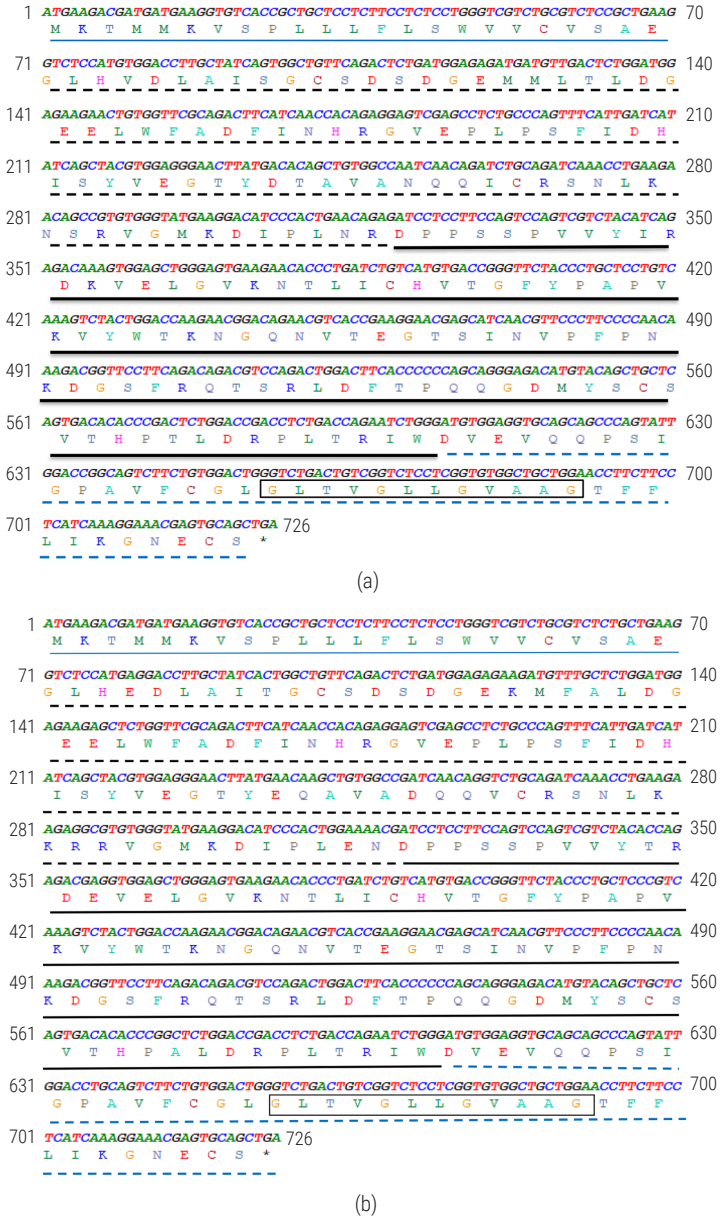

(a)

(b)

Fig 1. Coding DNA Sequence (CDS) of MHC II A in (a) *T. mookalee (Trmo-DAA)* and (b) *T. blochii (Trbl-DAA).* Nucleotide sequences of the coding region are shown in bold italics and the corresponding amino acid sequences indicated below. Start codon and the leader peptide sequences are underlined in blue. The α_1 domain is indicated in black dashed underline and the α_2 domain in black solid underline. The cytoplasmic domain, connecting peptide and the transmembrane domain of the protein are marked with blue dashed underline. The conserved GxxxGxxGxxxG motif is marked with a rectangle box and the stop codon is denoted by an asterisk (*)

and *Lates calcarifer,* both belonging to the order Carangiformes, indicating the phylogenetic relation between species of the same order. Pairwise sequence comparisons revealed that *Trmo-DAA* and *Trbl-DAA* shared 6–80% homology with MHC II A sequences from human and other teleosts, indicating variable levels of conservation, with higher similarity observed among teleost species and lower similarity with distantly related taxa. The observed conservation is primarily restricted to key functional domains, with considerable variability across the full-length sequences (Stet *et al.*, 2002; Srisapoome *et al.*, 2004; Buonocore *et al.*, 2007; Yu *et al.*, 2010; Xu *et al.*, 2011).

The phylogenetic tree obtained through maximum likelihood analysis (Fig. 3) clearly demonstrates that *T. mookalee* (*Trmo-DAA*) and *T. blochii* (*Trbl-DAA*) clustered closely with *T. ovatus*, forming a well supported clade within the family Carangidae. This clustering is supported by high bootstrap values, indicating strong evolutionary relatedness

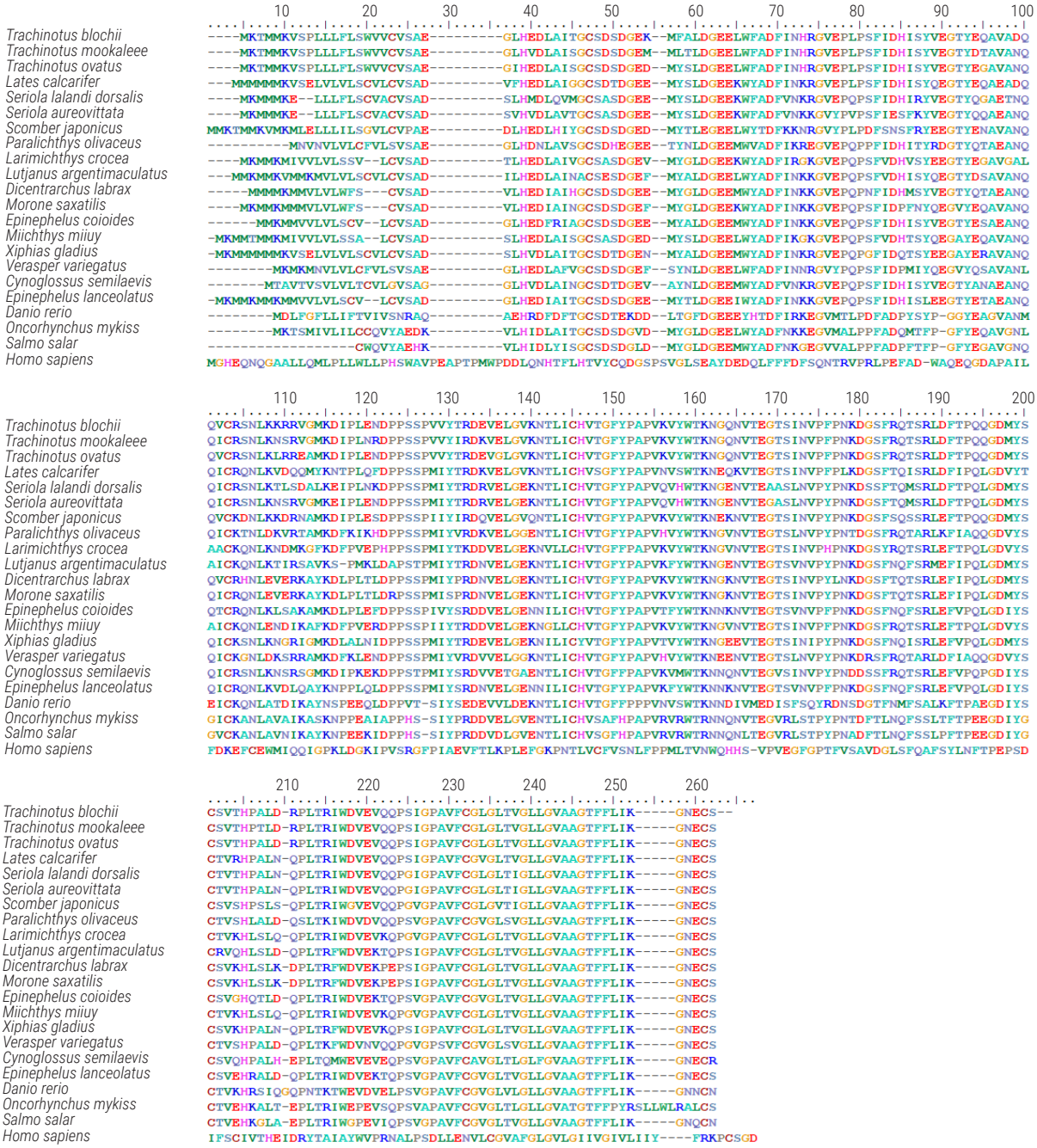

Fig. 2. Multiple sequence alignment of deduced amino acid sequences of MHC II A gene of *T. mookalee* and *T. blochii* with other teleosts and *Homo sapiens*. The alignment reveals conserved and variable regions across species

among *Trachinotus* species. Members of the family Scombridae and other related teleosts formed neighbouring clusters, whereas sequences from more distantly related teleost species and *Homo sapiens* formed separate clades, reflecting evolutionary divergence across taxa. The observed topology suggests that the MHC II A gene exhibits conservation within closely related species, particularly within Carangiformes, while showing divergence across distant lineages (Sato *et al.*, 2012). Such conservation within functional groups may facilitate the identification and mapping of polymorphic regions associated with disease resistance in *Trachinotus* species.

Sequence and functional analysis of *Trmo-DAA* and *Trbl-DAA* genes

In silico analysis employs computational tools to rapidly analyse genomic data, predict gene functions (such as binding sites, protein structure and regulatory elements), and model biological processes, thereby minimising the time and cost involved in experimental laboratory work. *In silico* analysis performed to characterise the molecular and functional features of *Trmo-DAA* and *Trbl-DAA* and the physico-chemical properties of both the proteins predicted using ExPasy ProtParam tool are given in Table 2. In *Trmo-DAA*, 22 phosphorylation sites were predicted comprising, Serine (Ser) - 11, Threonine (Thr) - 9 and Tyrosine (Tyr) - 2 residues, while in *Trbl-DAA*, 21 phosphorylation sites were identified including, Ser - 10, Thr - 9 and Tyr - 2. In both *Trachinotus* species, a single N-linked glycosylation site was identified at Asp150 within the α_2 domain of the protein; consistent with the observations in other teleosts such as golden pompano (Cao *et al.*, 2018), Japanese flounder (Xu *et al.*, 2010), turbot (Zhang *et al.*, 2006) and half-smooth tongue sole (Xu *et al.*, 2009). PSORT prediction indicated predominant protein localisation in the endoplasmic reticulum (44.4%), followed by the Golgi complex (33.3%) and plasma membrane (22.2%), for both species.

The InterProScan analysis (Fig. 4) classified both query sequences within the MHC class II family and identified key functional domains, including the MHC class II antigen-recognition domain and

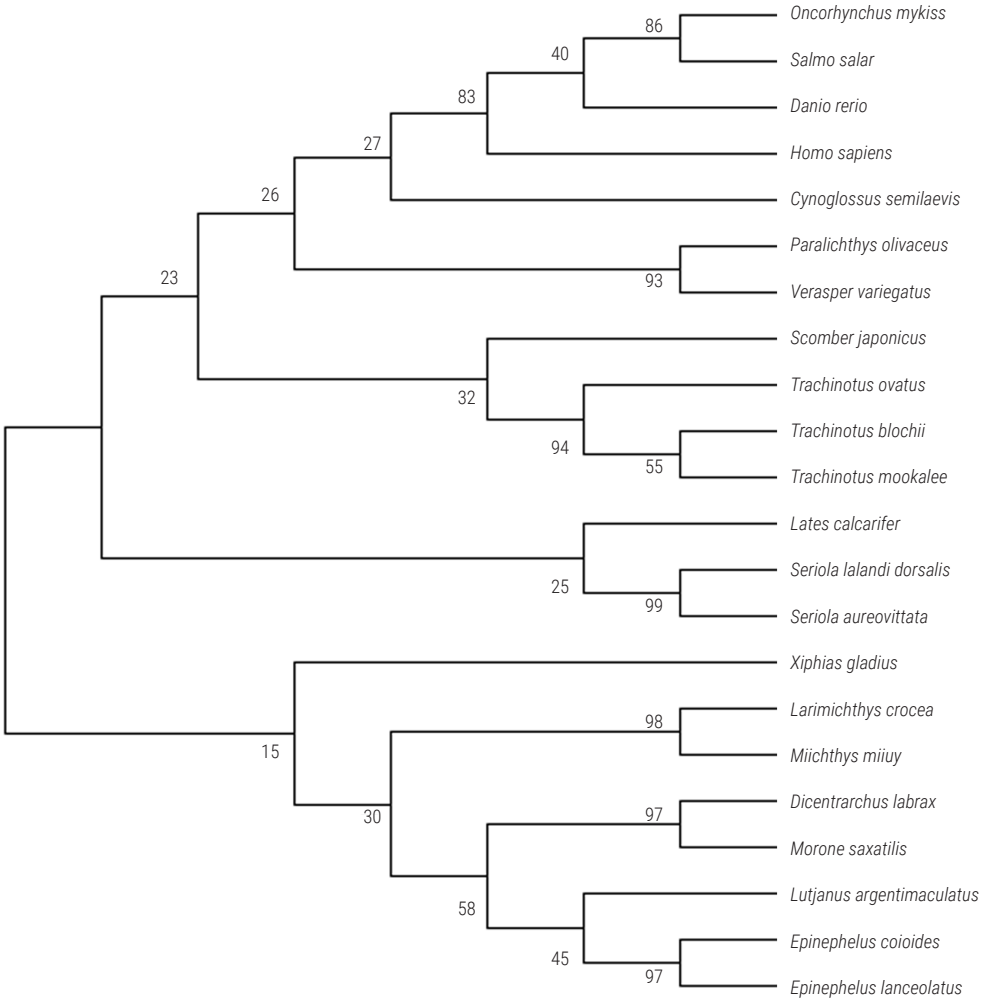

Fig. 3. Maximum likelihood phylogenetic tree of MHC II A amino acid sequences of *T. mookalee* and *T. blochii* along with representative teleosts and *Homo sapiens*. Bootstrap values (shown at the nodes) indicate branch support

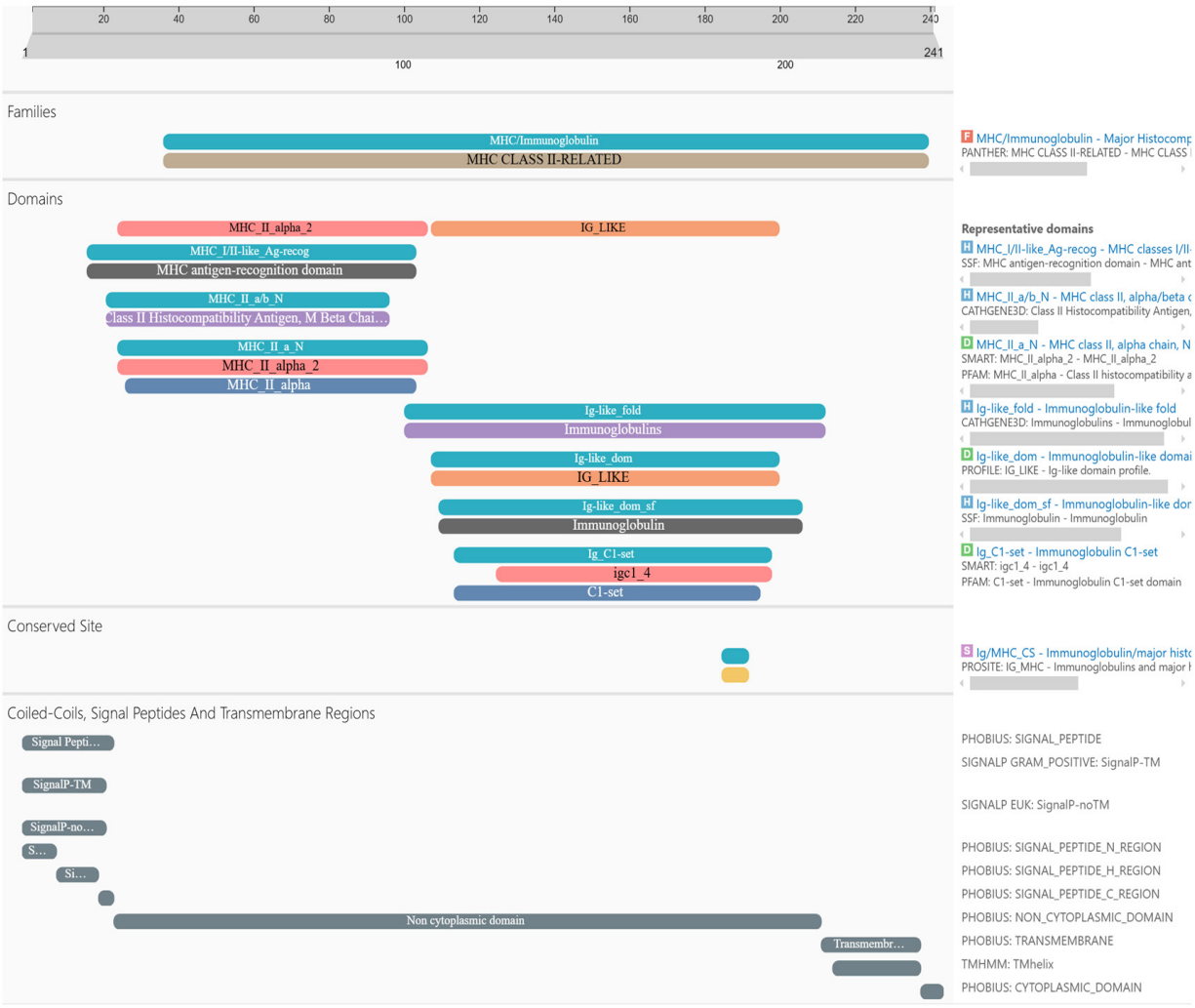

Fig. 4. Conserved domain and motif architecture of the MHC class II A protein predicted using InterProScan. The analysis identified conserved domains and functional motifs within the MHC class II A protein, including regions critical for peptide binding and immune recognition

the immunoglobulin like domain. A conserved immunoglobulin-MHC interaction site was identified at positions 184-190. The conserved GxxxGxxGxxxG motif was found at the cytoplasmic transmembrane region, *i.e.,* positions 219-230 of amino acid sequences in both the candidate species. This region is highly conserved in most vertebrates including teleosts, as it is found to be crucial for the interaction between MHC class II α and β chains (Cosson and Bonifacino, 1992). Structural topology prediction using Phobius identified the presence of signal peptides at positions 1-24 in *Trmo-DAA* and 1-22 in *Trbl-DAA*. The non-cytoplasmic domain was identified at positions 25-209 in *Trmo-DAA* and 23-209 in *Trbl-DAA*. The transmembrane region was identified at positions 210-235, and the cytoplasmic domain at positions 236-241 in both proteins. The transmembrane protein structures plotted by online tool Protter are depicted in Fig. 5a, b.

The STRING database was used to construct the protein-protein interaction network for the given candidate genes based on seven distinct channels such as neighbourhood, gene fusion, co-occurrence, co-expression, experimental data, databases and text mining. The resulting network Fig. 6a indicated strong interactions of the query protein with key immune-related molecules, particularly CD74 (MHC class II invariant chain), which exhibited the highest similarity score (0.953) along with other MHC class II-associated proteins. The enrichment analysis for Gene Ontologies (GO) based on biological processes (Fig. 6b) showed that the *Trmo-DAA* and *Trbl-DAA* are mainly involved in antigen processing and presentation of exogenous antigens *via* MHC class II complex. KEGG pathway enrichment analysis (Fig. 6c) further demonstrated the involvement of these genes in pathways such as the intestinal immune network for antibody (IgA) production and in pathways related to cell adhesion molecules, highlighting their role in mucosal immunity and immune cell interactions. The physico-chemical properties of MHC II A protein in both fish species (Table 2) were consistent with those reported for major teleost fishes like grass carp, Nile tilapia, zebra fish, rainbow trout and channel catfish (Tuan and Duc, 2016), reflecting evolutionary conservation of this immune gene across teleosts.

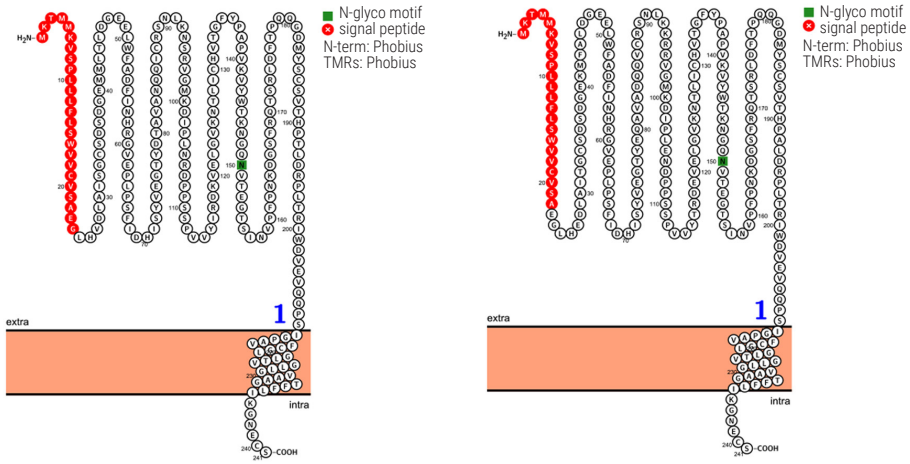

Fig. 5. Topological organisation of MHC class II A in (a) *T. mookalee* and (b) *T. blochii,* predicted using Protter tool. Protter output shows the positions of the signal peptides, transmembrane regions and functional domains. Domains located in cytoplasmic, non-cytoplasmic (extracellular), and transmembrane regions are clearly indicated, providing insights into the structural organisation and membrane orientation of the MHC class II A protein.

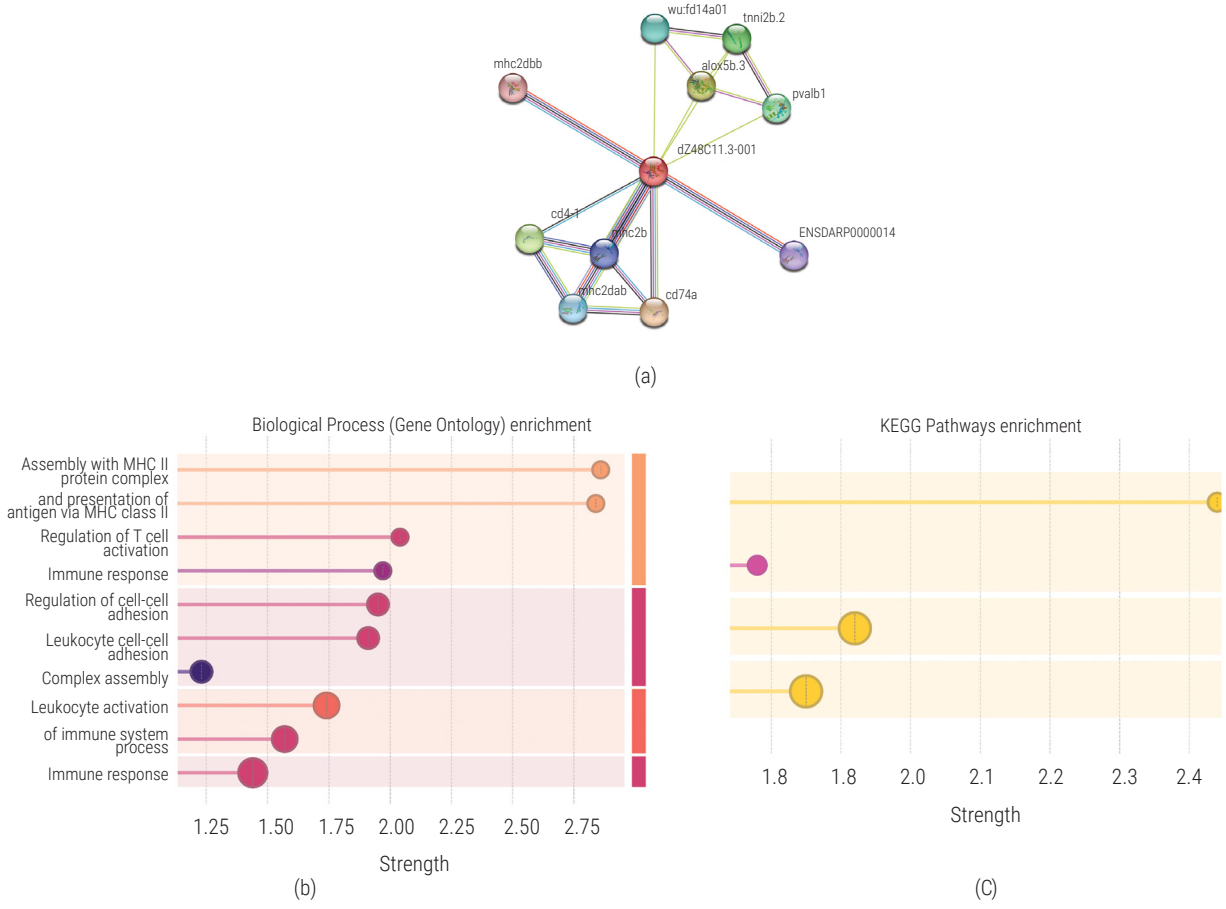

Fig. 6. (a) Protein-protein interaction network of MHC II A protein predicted using STRING database, showing associations with immune related proteins. Nodes represent proteins, while edges indicate the predicted interactions. (b) Graphical representation on the enrichment analysis for Gene Ontologies based on biological process for *Trmo-DAA* and *Trbl-DAA*. Bar graph represents the enriched biological processes associated with the *Trmo-DAA* and *Trbl-DAA* proteins. Each bar corresponds to a GO term and the length of the bar indicates the level of enrichment or significance. (c) KEGG pathways enrichment analysis graph for *Trmo-DAA* and *Trbl-DAA*. Bar graph shows the enriched KEGG pathways associated with *Trmo-DAA* and *Trbl-DAA*, highlighting the biological pathways in which these proteins are potentially involved. Each bar represents a specific pathway, with the length indicating the level of enrichment or statistical significance

Table 2. Physico-chemical properties of the predicted *Trmo-DAA* and *Trbl-DAA* MHC II A proteins

Protein	No. of amino acids	Molecularweight (KDa)	Theoretical pI	Instability index	Aliphatic index	Grand average hydropathy (GRAVY) score
Trmo-DAA	241	265.05	5.33	36.36 (stable)	87.63	-0.02
Trbl-DAA	241	265.93	5.01	42.76 (> 40 - unstable)	83.61	-0.104

Secondary and tertiary structure prediction of *Trmo-DAA* and *Trbl-DAA*

The secondary structure of *Trmo-DAA* and *Trbl-DAA* proteins, *i.e.* coiled coils, helices and strands predicted using PSIPRED 4.0 and Phyre 2.2 are given in Fig. 7a and b, respectively, which revealed a similar structural organisation in both species, with coiled coils and β-strands forming the major components. The helices were mainly found in the signal peptides and transmembrane regions. This pattern is consistent with MHC II A proteins in other teleosts, such as zebrafish, channel catfish, Nile tilapia and rainbow trout, where random coils predominate, followed by β-strands (Tuan and Duc, 2016).

Template search for three-dimensional (3D) structure prediction of query *Trmo-DAA* and *Trbl-DAA* amino acid sequences performed using SWISS-MODEL presented 50 hits. Among these, the AlphaFold DB model A0A4W6CS56 of *L. calcarifer* (barramundi) showing the highest sequence identity and coverage, of 78.42% for *Trmo-DAA* and 79.67% for *Trbl-DAA*, was selected as the template for homology modelling of 3D structure.

The structural assessment of the predicted 3D structure (Fig. 8a) was done *via* Ramachandran plot and MolProbity scores. Lower MolProbity scores indicated better model quality; accordingly, *Trbl-DAA* had a slightly better score (1.16) compared to *Trmo-DAA* (1.41) (Table 3). Ramachandran plot analysis revealed that 94.98% of residues occupied favoured regions in both predicted structures (Fig. 8b), confirming good stereochemical quality and reliability of the modeled 3D structures. Proline and Glycine residues are at times encountered as Ramachandran outliers, and the single Ramachandran outlier present in these structure models is a Proline residue, which is acceptable as an exception. The conserved immunoglobulin-like fold characteristic of MHC II A proteins, comprising two extracellular domains with β-sheet organisation, a connecting peptide, a transmembrane region and a cytoplasmic tail, was also observed in *Trmo*-DAA (Fig. 8a).

Fig. 7 (a) Secondary structure of the protein generated using PSIPRED server. Cartoon illustration shows the arrangement of secondary structural elements, including α-helices, β-strands, and coiled (loop) regions. The prediction provides a visual representation of the peptide's structural features, highlighting regions of potential stability and flexibility that may influence its function and interactions

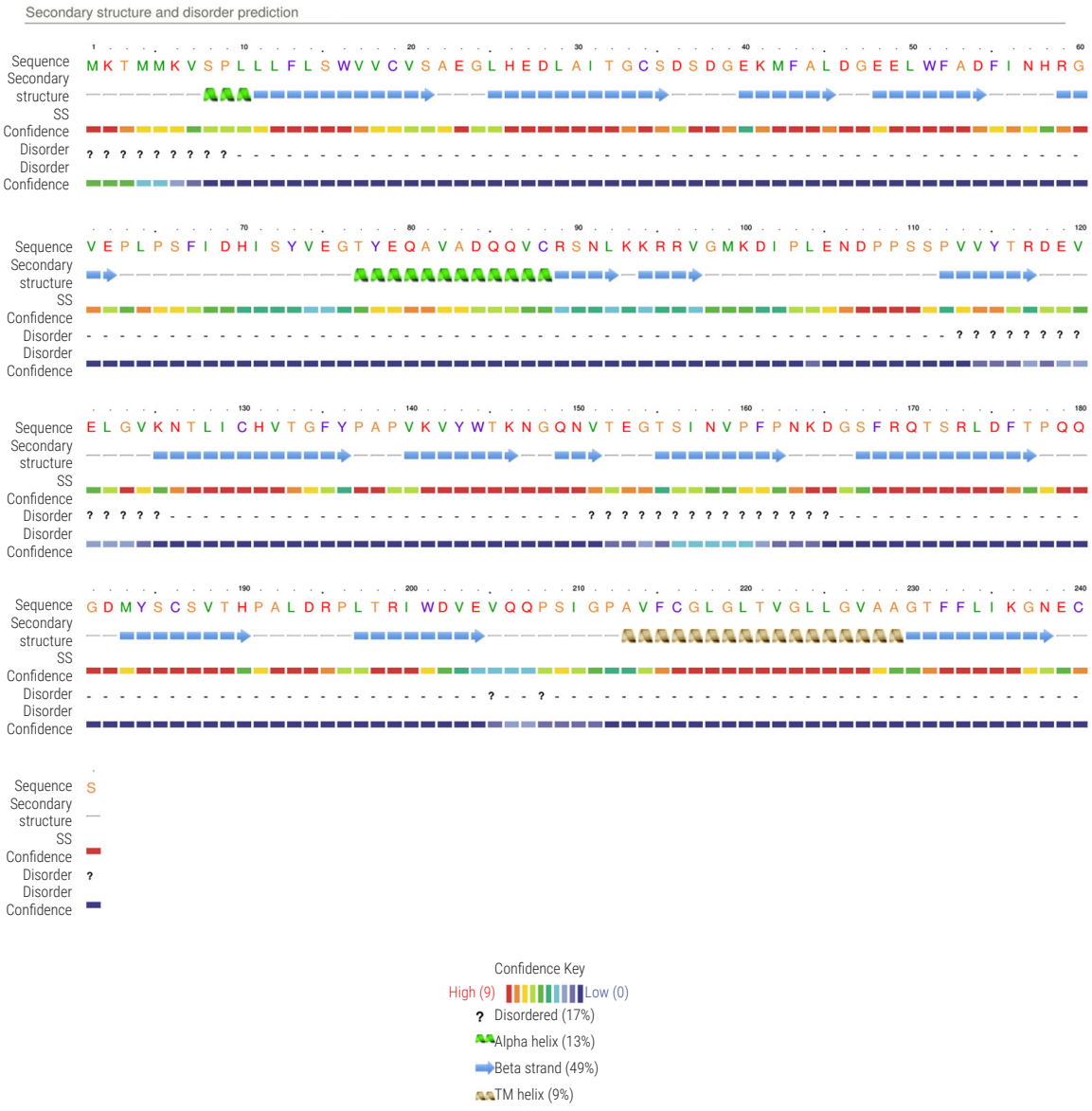

Fig. 7 (b) Secondary structure of the protein generated using Phyre2.2. which illustrates the arrangement of secondary structural elements, including α-helices, β-strands, and transmembrane helices. The representation highlights the spatial organisation of these elements, providing insights into the structural features, membrane orientation and potential functional regions of the protein

Table 3. MolProbity validation results for the predicted 3D structures of *Trmo-DAA* and *Trbl-DAA* proteins

Assessment features	*Trmo-DAA*	*Trbl-DAA*
MolProbity score	1.41	1.16
Clash score	2.71	1.08
Ramachandran favoured	94.98%	94.98%
Ramachandran outliers (A112 PRO)	0.42%	0.42%
Rotamer outliers (A14 LEU, A42 MET)	0.94%	0.95%
C-Beta deviations (A8 SER)	1	1
Bad bonds	0 / 1907	0 / 1916
Bad angles	16 / 2599	13 / 2609
Cis prolines	2 / 16	2 / 16

The Phyre-2.2 server also predicted 3D structures for the *Trmo-DAA* and *Trbl-DAA* sequences based on the most appropriate AlphaFold model as template. The *Trmo-DAA* structure was modeled using template c7t6iA, corresponding to the human leukocyte antigen (HLA) class II DP α chain, with 99.94% confidence (Fig. 9a). The *Trbl-DAA* model constructed using the template c4x5wA corresponding to HLA-DR1 with CLIP102-120 mutant (m107w) from *Homo sapiens,* showed 99.95% confidence (Fig. 9b).

Ramachandran analysis for the predicted 3D structure showed six residues in *Trmo-DAA* and two residues in *Trbl-DAA*, falling within disallowed regions (shown in red in Fig. 9c and d), indicating minor deviations but with overall acceptable stereochemical quality.

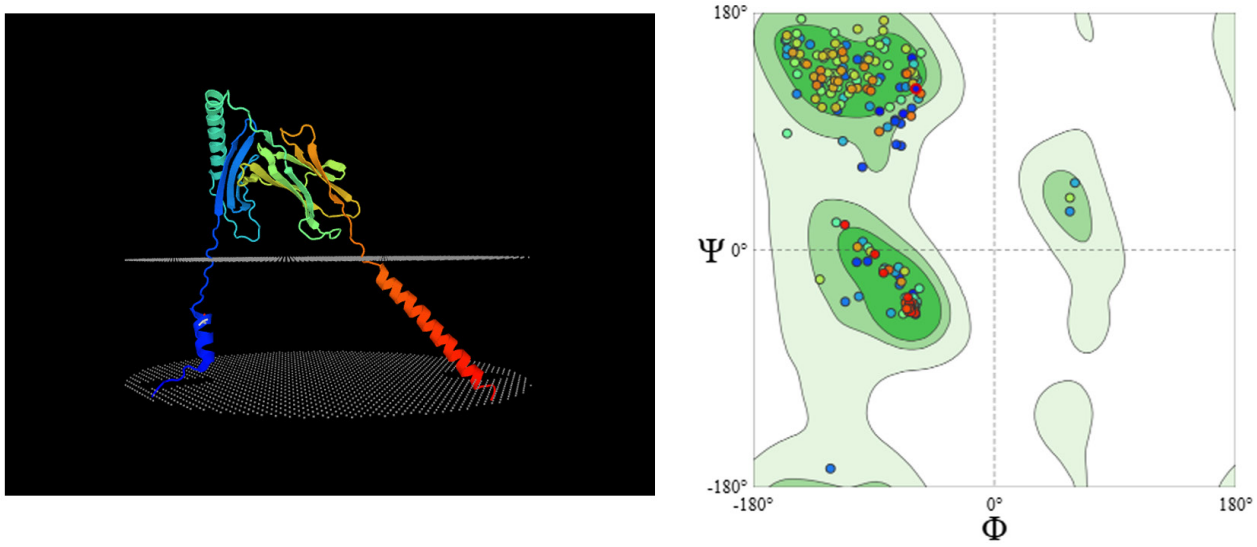

(a) (b)

Fig. 8. (a) The three-dimensional (3D) structure of the target protein estimated using SWISS-MODEL, with the AlphaFold DB structure A0A4W6CS56 of *L. calcarifer* as the template; (b) Ramachandran plot for the validation of the 3D structure. The Ramachandran plot was generated to assess the stereochemical quality of the modeled protein structure obtained through homology modeling

Active site prediction using fpocket2 tool in Phyre-2.2 identified prominent ligand-binding pockets in both structures (Fig. 9e and f). These pockets, visualised in wireframe mode and highlighted in red, are primarily located in the peptide binding regions and may contribute to the functional variability of MHC class II molecules which is linked to disease resistance in most teleost fishes.

A comparison of the 3D structures predicted by the two online tools revealed that the primary variation arises from the template selected for prediction. The SWISS-MODEL templates showed higher sequence similarity (78-80%) with the query sequence, while the Phyre-2.2 templates showed comparatively lower (73-74%) similarity, although both approaches produced structurally consistent models.

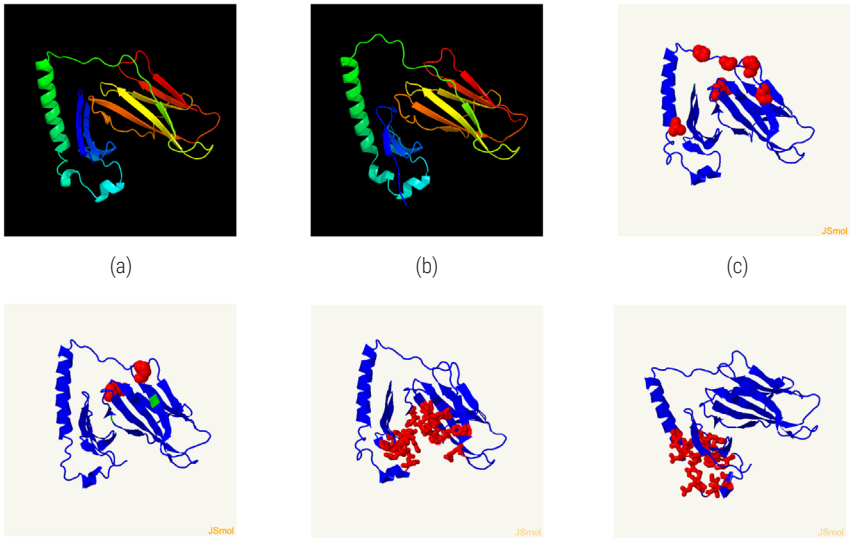

(a) (b) (c)

(d) (e) (f)

Fig. 9. Predicted 3D structure of (a) *Trmo-DAA* generated using Phyre2.2 (template c7t6iA; 99.94% confidence in structural similarity); (b) *Trbl-DAA* generated using the Phyre2.2 (template c4x5wA; 99.95% confidence). (c, d) Ramachandran plot analysis of the predicted 3D structure of *Trmo-DAA* and *Trbl-DAA*, respectively, showing the majority of residues within allowed regions (shown in blue), with a few residues in disallowed regions (highlighted in red), indicating acceptable stereochemical quality. (e, f) Predicted active site pockets of *Trmo-DAA* and *Trbl-DAA* respectively, identified using fpocket2 in Phyre2.2, with the 3D structures shown in wireframe mode and potential ligand-binding regions highlighted in red

The structure predicted by SWISS-MODEL showed a transmembrane region, which was not evident in the structure predicted by Phyre 2.2. The Phyre-2.2 predicted structures exhibited high (99%) confidence in similarity with the crystal structure of the templates used. Ramachandran plot validation of the predicted structures indicated that the *Trbl-DAA* 3D structure possessed slightly better stereochemical quality than *Trmo-DAA*, suggesting a more stable and reliable model. The 3D structures predicted using both SWISS-MODEL and Phyre 2.2 provide complementary structural insights and facilitate a better understanding of the molecular architecture of *Trmo-DAA* and *Trbl-DAA* proteins. Based on the validated results obtained from the Ramachandran plot and MolProbity score, the predicted 3D models for MHC II A protein of the *Trachinotus* species in the current study can be trusted and accepted. These models may serve as useful references for future experimental studies aimed at determining the crystal structures of MHC II A proteins. However, previous studies have reported the presence of multiple loci of the MHC class II A gene in various teleost species (Zhang and Chen 2006; Xu *et al.* 2009; Li *et al.* 2011), suggesting possible genetic diversification within this gene family across species.

The results of the current study on the physico-chemical properties, molecular functions and structural organisation of the MHC II A gene in *T. mookalee* and *T. blochii* provide a foundation for future investigations into genetic variations associated with disease resistance in these species. This study provides the first insights into the genetic organisation and *in silico* characterisation of the MHC II A gene in *T. mookalee* and *T. blochii*. Further studies on gene polymorphisms linked to disease resistance may facilitate the development of marker-assisted selective breeding and genetic improvement programs aimed at enhancing immune competence and overall resilience of these two commercially important pompano species.

Acknowledgements

Research was supported by the Indian Council of Agricultural Research (ICAR), Department of Agricultural Research and Education, Government of India. The authors are grateful to the Director, ICAR-CMFRI, Kochi for the financial support and encouragement provided to carry out the research work. The authors also acknowledge Dr. Dileep Vasudevan, Scientist F, BRIC-Rajiv Gandhi Centre for Biotechnology (BRIC-RGCB) for his valuable insights and recommendations on the structural modelling of the gene.

References

Amal, M. N. A., Zamri-Saad, M., Iftikhar, A. R., Siti-Zahrah, A., Aziel, S. and Fahmi, S. 2012. An outbreak of *Streptococcus agalactiae* infection in cage-cultured golden pompano, *Trachinotus blochii* in Malaysia. *J. Fish. Dis.,* 35: 849–852. https://doi.org/10.1111/j.1365-2761.2012.01443.x.

Apanius, V., Penn, D., Slev, P. R. and Ruff, L. R. 1997. The nature of selection on the major histocompatibility complex. *Crit. Rev. Immunol*., 17: 179-224. https://doi.org/10.1615/critrevimmunol.v17.i2.40.

Bannai, H. P. and Nonaka, M. 2013. Comprehensive analysis of medaka major histocompatibility complex (MHC) class II genes: Implications for evolution in teleosts. *Immunogenetics*, 65: 883–895. https://doi.org/10.1007/s00251-013-0731-8.

Brown, J. H., Jardetzky, T. S., Gorga, J. C. and Stern, L. J. 1993. Three-dimensional structure of the human class II histocompatibility antigen HLA-DR1. *Nature,* 364: 33-39. https://doi.org/10.1038/364033a0.

Buonocore, F., Randelli, E., Casani, D., Costantini, S., Facchiano, A., Scapigliati, G. and Stet, R. J. 2007. Molecular cloning, differential expression and 3D structural analysis of the MHC class-II beta chain from sea bass (*Dicentrarchus labrax* L.). *Fish Shellfish Immunol*., 23(4): 853–866. https://doi.org/10.1016/j.fsi.2007.03.013.

Cao, Z., Wang, L., Xianga, Y., Liu, X., Tu, Z., Sun, Y. and Zhou, Y. 2018. MHC class IIα polymorphism and its association with resistance/ susceptibility to *Vibrio harveyi* in golden pompano (*Trachinotus ovatus*). *Fish Shellfish Immunol*., 80: 302–310. https://doi.org/10.1016/j.fsi.2018.06.020.

Chavez, H. M., Fang, A. L. and Carandang, A. A. 2011. Effect of stocking density on growth performance, survival and production of silver pompano, *Trachinotus blochii* (Lacepede, 1801) in marine floating cages. *Asian Fish. Sci.,* 24: 321-330, https://doi.org/10.33997/j.afs.2011.24.3.005.

Chen, J., Zheng, Y., Zhi, T., Xu, X., Zhang, S., Brown, C. L. and Yang, T. 2021. MHC II α polymorphism of Nile tilapia, *Oreochromis niloticus*, and its association with the susceptibility to *Gyrodactylus cichlidarum* (Monogenea) infection. *Aquaculture,* 539(736637): 1-8. https://doi.org/10.1016/j.aquaculture.2021.736637.

Cosson, P. and Bonifacino, J. S. 1992. Role of transmembrane domain interactions in the assembly of class II MHC molecules. *Science,* 258: 659. https://doi.org/10.1126/science.1329208.

Eizaguirre, C., Lenz, T. L., Kalbe, M. and Milinski, M. 2012. Rapid and adaptive evolution of MHC genes under parasite selection in experimental vertebrate populations. *Nat. Commun.,* 3: 621. https://doi.org/10.1038/ncomms1632.

Gjedrem, T., Salte, R. and Gjoen, H. M. 1991. Genetic variation in susceptibility of Atlantic salmon to furunculosis. *Aquaculture,* 97: 1–6. https://doi.org/10.1016/0044-8486(91)90274-B.

Glamann J. 1985. Complete coding sequence of rainbow trout MHC II B chain. *Scand. Immunol.,* 41: 365-372. https://doi.org/10.1111/j.1365-3083.1995.tb03580.x.

Glover, K. A., Grimholt, U., Bakke, H. G., Nilsen, F., Storset, A. and Skaala, O. 2007. Major histocompatibility complex (MHC) variation and susceptibility to the sea louse *Lepeophtheirus salmonis* in Atlantic salmon *Salmo salar*. *Dis. Aquat. Organ*., 76: 57–65. https://doi.org/10.3354/dao076057.

Godwin, U. B., Antao, A., Wilson, M. R., Chinchar, V. G., Miller, N. W., Clem, L. W. and McConnell, T. J. 1997. MHC class II B genes in the channel catfish (*Ictalurus punctatus*). *Dev. Comp. Immunol*., 21(1): 13–23. https://doi.org/10.1016/S0145-305X (97)00003-7. https://doi.org/10.1016/s0145-305x(97)00003-7.

Gopakumar, G., Abdul Nazar, A. K., Jayakumar, R., Tamilmani, G., Kalidas, C., Sakthivel, M., Rameshkumar, P., Rao, G. H., Premjothi, R., Balamurugan, V., Ramkumar, B., Jayasingh, M. and Rao, G. S. 2012. Broodstock development through regulation of photoperiod and controlled breeding of silver pompano, *Trachinotus blochii* (Lacepede, 1801) in India. *Indian J. Fish*., 59: 53–57.

Grimholt, U., Larsen, S., Nordmo, R., Midtlyng, P., Kjoeglum, S., Storset, A., Saebo, S. and Stet, R. J. M. 2003. MHC polymorphism and disease resistance in Atlantic salmon (*Salmo salar*); facing pathogens with single expressed major histocompatibilty class I and class II loci. *Immunogenetics*, 55: 210-219. https://doi.org/10.1007/s00251-003-0567-8.

Grimholt, U., Olsaker, I., Lindstrom, C. V. and Lie, O. 1994. A study of variability in the MHC class II _1 and class I _2 domain exons of Atlantic salmon (*Salmo salar*). *Anim. Genet*., 25: 147–153. https://doi.org/10.1111/j.1365-2052.1994.tb00103.x.

Hardee, J. J., Godwin, U., Benedetto, R. and McConnell, T. J. 1995. Major histocompatibility complex class II A gene polymorphism in the striped bass. *Immunogenetics*, 41: 229-238. https://doi.org/10.1007/BF00172064.

Hordvik, I., Grimholt, U., Fosse, V. M., Lie, O. and Endresen, C. 1993. Cloning and sequence analysis of cDNAs encoding the MHC class II ß chain in Atlantic salmon (*Salmo salar*). *Immunogenetics*, 37: 437-441. https://doi.org/10.1007/BF00222467.

Jiang, J., Li, C., Zhang, Q. and Wang, X. 2013. Cloning and characterization of major histocompatibility complex class II genes in the stone flounder *Kareius bicoloratus* (Pleuronectidae). *Genet. Mol. Res*., 12(4): 5820-5832. https://doi.org/10.4238/2013.

Klein, J. and Figueroa, F. 1986. Evolution of the major histocompatibility complex. *Crit. Rev. Immunol*., 6: 295-386.

Klein, J., Bontrop, R. E., Dawkins, R. L., Erlich, H. A., Gyllensten, U. B., Heise, E. R., Jones, P. P., Parham, P., Wakeland, E. K. and Watkins, D. I. 1990. Nomenclature for the major histocompatibility complexes of different species: A proposal. *Immunogenetics*, 31: 217–219. https://doi.org/10.1007/BF00204894.

Kumar, R. P., Abdul Nazar, A. K., Jayakumar, R., Tamilmani, G., Sakthivel, M., Kalidas, C., Balamurugan, V., Sirajudeen, S., Thiagu, R. and Gopakumar, G. 2015. *Amyloodinium ocellatum* infestation in the broodstock of silver pompano *Trachinotus blochii* (Lacepede, 1801) and its therapeutic control. *Indian J. Fish*., 62(1): 131-134.

Li, C., Yu, Y., Sun, Y. and Li, S. 2010. Isolation, polymorphism and expression study of two distinct major histocompatibility complex class II B genes from half-smooth tongue sole (*Cynoglossus semilaevis*). *Int. J. Immunogenet*., 37: 185-197. https://doi.org/10.1111/j.1744-313X.2010.00909.x.

Li, H., Jiang, L., Han, J., Su, H., Yang, Q. and He, C. 2011. Major histocompatibility complex class IIA and IIB genes of the spotted halibut *Verasper variegatus*: Genomic structure, molecular polymorphism, and expression analysis. *Fish Physiol. Biochem*., 37(4): 767–780. https://doi.org/10.1007/s10695-011-9476-1.

Li, X., Du, H., Liu, L., You, X., Wu, M. and Liao, Z. 2017. MHC class II alpha, beta and MHC class II-associated invariant chains from Chinese sturgeon (*Acipenser sinensis*) and their response to immune stimulation. *Fish Shellfish Immunol*., 70: 1–12. https://doi.org/ 10.1016/j.fsi.2017.08.042.

Lohm, J., Grahn, M., Langefors, A., Andersen, O., Storset, A. and Schantz, T. 2002. Experimental evidence for major histocompatibility complex-allele-specific resistance to a bacterial infection. *Proc. Biol. Sci*., 69: 2029–2033. https://doi.org/10.1098/rspb.2002.2114.

Ono, H., Klein, D., Vincek, V., Figueroea, F., O'hUigin, C., Tichy, H. and Klein, J. 1992. Major histocompatibility complex class II genes of zebrafish. *Proc. Natl. Acad. Sci. USA*, 89: 11886-11890. https://doi.org/10.1073/pnas.89.24.11886.

Pang, J., Gao, C., Lu, M., Ye, X., Zhu, H. and Ke, X. 2013. Major histocompatibility complex class IIA and IIB genes of Nile tilapia *Oreochromis niloticus*, genomic structure, molecular polymorphism and expression patterns. *Fish Shellfish Immunol*., 34: 486-496. https://doi.org/10.1016/j.fsi.2012.11.048.

Powell, H. R., Islam, S. A., David, A. and Sternberg, M. J. E. 2025. Phyre2.2: A community resource for template-based protein structure prediction. *J. Mol. Biol*., 437(15): 168960. https://doi.org/10.1016/j.jmb.2025.168960.

Rakus, K. L., Wiegertjes, G. F., Adamek, M., Siwicki, A. K., Lepa, A. and Irnazarow, I. 2009a. Resistance of common carp (*Cyprinus carpio* L.) to cyprinid herpesvirus-3 is influenced by major histocompatibility (MH) class II B gene polymorphism. *Fish Shellfish Immunol*., 26: 737–743. https://doi.org/10.1016/j.fsi.2009.03.001.

Rakus, K. L., Wiegertjes, G. F., Jurecka, P., Walker, P. D., Pilarczyk, A. and Irnazarow, I. 2009b. Major histocompatibility (MH) class II B gene polymorphism influences disease resistance of common carp (*Cyprinus carpio* L.). *Aquaculture*, 288: 44–50. https://doi.org/10.1016/j.aquaculture.2008.11.016.

Ransangan, J., Manin, B. O., Abdullah, A., Roli Z. and Sharudin, E. F. 2011. Betanodavirus infection in golden pompano, *Trachinotus blochii*, fingerlings cultured in deep-sea cage culture facility in Langkawi, Malaysia. *Aquaculture,* 315: 327–334. https://doi.org/10.1016/j.aquaculture.2011.02.040.

Rothbard, J. B. and Gefter, M. L. 1991. Interactions between immunogenic peptides and MHC proteins. *Ann. Rev. Immunol.,* 9: 527-565. https://doi.org/10.1146/ annurev.iy.09.040191.002523.

Sambrook, J. and Russell, D. W. 2001. *Molecular cloning: A laboratory manual*, Vol. 1, 3rd edn. , Cold Spring Harbor Laboratory Press, New York, USA.

Sato, A., Dongak, R., Hao, L., Shintani, S. and Sato, T. 2012. Organization of MHC class II A and B genes in the tilapiine fish *Oreochromis*. *Immunogenetics*, 64: 679–690.

Sekar, M., Ranjan, R., Xavier, B., Ghosh, S., Pankyamma, V., Ignatius, B., Joseph, I. and Achamveetil, G. 2021. Species validation, growth, reproduction and nutritional perspective of Indian pompano, *Trachinotus mookalee*: A candidate species for diversification in coastal mariculture. *Aquaculture*, 545: 737212. https://doi.org/10.1016/j.aquaculture.2021.737212.

Spurgin, L. G. and Richardson, D. S. 2010. How pathogens drive genetic diversity: MHC, mechanisms and misunderstandings. *Proc. Biol. Sci*., 277: 979–988. https://doi.org/10.1098/rspb.2009.2084.

Srisapoome, P., Ohira, T., Hirono, I. and Aoki, T. 2004. Cloning, characterization and expression of cDNA containing major histocompatibility complex class I, IIα and IIβ genes of Japanese flounder. *Fish. Sci*., 70(2): 264–276. https://doi.org/10.1111/j.1444-2906.2003.00800.

Stet, R. J., de Vries, B., Mudde, K., Hermsen, T., van Heerwaarden, J., Shum, B. P. and Grimholt, U. 2002. Unique haplotypes of co-segregating major histocompatibility class II A and class II B alleles in Atlantic salmon (*Salmo salar*) give rise to diverse class II genotypes. *Immunogenetics,* 54: 320–331. https://doi.org/10.1007/s00251-002-0477-1.

Sultmann, H., Mayer, W. E., Figueroea, F., O'hUigin, C. and Klein, J. 1993. Zebrafish MHC class II a chain-encoding gene: Polymorphism, expression and function. *Immunogenetics*, 38: 408-420. https://doi.org/10.1007/BF00184521.

Tuan T. N. and Duc, P. M. 2016. *In silico* analysis of freshwater fish major histocompatibility complex class II alpha. *Asia-Pacific J. Sci. Technol.,* 21: 4, APST–21. https://doi.org/10.14456/apst.2016.18.

Van Erp, S. H. M., Egberts, E. and Stet, R. J. M. 1996. Characterization of class II A and B genes in a gynogenetic carp clone. *Immunogenetics*, 44: 192-202. https://doi.org/10.1007/BF02602585.

Walker, R. A. and McConnell, T. J. 1994. Variability in an MHC class II b chain-encoding gene in striped bass (*Morone saxatilis*). *Dev. Comp. Immunol*., 18: 325-342. https://doi.org/10.1016/s0145-305x(94)90358-1.

Wynne, J. W., Cook, M. T., Nowak, B. F. and Elliott, N. G. 2007. Major histocompatibility polymorphism associated with resistance towards amoebic gill disease in Atlantic salmon (*Salmo salar* L.). *Fish Shellfish Immunol*., 22: 707-717. https://doi.org/10.1016/j.fsi.2006.08.019.

Xu, T., Chen, S. L. and Zhang Y. X. 2010. MHC class II alpha gene polymorphism and its association with resistance/susceptibility to *Vibrio anguillarum* in Japanese flounder (*Paralichthys olivaceus*). *Dev. Comp. Immunol*., 34: 1042–1050. https://doi.org/10.1016/j.dci.2010.05.008.

Xu, T., Sun, Y., Shi, G. and Cheng, Y. 2011. Characterization of the major histocompatibility complex class II genes in *miiuy croaker*. *PLoS ONE*, 6: e23823. https://doi.org/10.1371/journal.pone.0023823.

Xu, T., Chen, S., Ji, X. and Sha, Z. 2009. Molecular cloning, genomic structure, polymorphism and expression analysis of major histocompatibility complex class IIA and IIB genes of half-smooth tongue sole (*Cynoglossus semilaevis*). *Fish Shellfish Immunol*., 27: 192–201. https://doi.org/10.1016/j.fsi.2009.04.009.

Yang, M., Wei, J., Li, P., Wei, S., Huang, Y. and Qin, Q. 2016a. MHC polymorphism and disease resistance to Singapore grouper iridovirus (SGIV) in the orange-spotted grouper, *Epinephelus coioides*. *Sci. Bull*., 61: 693-699. https://doi.org/10.1016/j.fsi.2025.110571.

Yang, M., Wei, J., Li, P., Wei, S., Huang, Y. and Qin, Q. 2016b. MHC class II alpha polymorphisms and their association with resistance/susceptibility to Singapore grouper iridovirus (SGIV) in orange-spotted grouper, *Epinephelus coioides*. *Aquaculture,* 462: 10–16. https://doi.org/10.1016/j.aquaculture.2016.04.026.

Yang, Z., Yue, G. H. and Wong, S. M. 2022. VNN disease and status of breeding for resistance to NNV in aquaculture. *Aquac. Fish*., 7(2): 147-157. https://doi.org/10.1016/j.aaf.2021.04.001.

Yu, S. H., Ao, J. Q. and Chen, X. H. 2010. Molecular characterization and expression analysis of MHC class II alpha and beta genes in large yellow croaker (*Pseudosciaena crocea*). *Mol. Biol. Rep*., 37: 1295–1307. https://doi.org/10.1007/s11033-009-9504-8.

Zhang, Y. X. and Chen, S. L. 2006. Molecular identification, polymorphism, and expression analysis of major histocompatibility complex class II A and B genes of turbot (*Scophthalmus maximus*). *Mar. Biotechnol*., 8(6): 611–623. https://doi.org/10.1007/s10126-005-6174-y.

Zhou, F., Dong, Z., Fu, Y., Li, T., Zeng, Y., Ji, X., Chen, W., Zhang, J. and Wang, H. 2013. Molecular cloning, genomic structure, polymorphism and expression analysis of major histocompatibility complex class II B gene of Nile tilapia (*Oreochromis niloticus*). *Aquaculture*, 372–375: 149–157. https://doi.org/10.1016/j.aquaculture.2012.10.032.

Zhu, K., Yu, W., Guo, H., Zhang, N., Jiang, S. and Zhang, D. 2018. The polymorphisms of MHC II beta gene of *Trachinotus ovatus* and their association with resistance/susceptibility to *Photobacterium damselae*. *Aquaculture*, 485: 160–165. https://doi.org/10.1016/j. aquaculture.2017.11.045.